Advanced Research in Fluid Mechanics and Thermal Sciences

An Experimental Study on Structure of Jet Injected into Crossflow

Open Access

Ni-oh Puzu[1,*] , Suteera Prasertsan[1], Makatar Wae-hayee[1], Chayut Nuntadusit[1]

[1]   Department of Mechanical Engineering, Faculty of Engineering, Prince of Songkhla University, Songkhla, Thailand

ARTICLE INFO	ABSTRACT
	Flow characteristics of a circular jet which was injected normal into the crossflow on flat plate, has been investigated by temperature measurement and flow visualization. The effect of jet-crossflow momentum flux ratio on jet flow behavior was studied by fixing the crossflow velocity and changing the velocity of jet flow. The experimental study was divided in two parts. First part, the flow visualization was done in water tunnel using Laser Induced Fluorescence (LIF) technique. Second part, the temperature of air jet flow was quantitatively measured with thermocouples and visualized the jet flow trajectory with smoke technique. The jet flow after injecting into crossflow had dome-shape structure and attached to the downstream surface for case of jet-crossflow momentum flux ratio less than 0.25. The results showed that the dome-shape structure was observed at the near field, while the Counter Rotating Vortex Pairs, CRVP appeared after that. When the jet was deep penetrated into the crossflow and moved away from the surface, which indicated jet-crossflow momentum flux ratio higher than 1.0, the jet flow had kidney-shape cross section and CRVP suddenly occurred in jet cross section behind the jet exit.

1. Introduction

The phenomena of jet injecting to the crossflow (jet in crossflow, JICF) are frequently encountered both in a nature and industry, ranging from flume dispersion to rocket controller. In a vast variety of applications, the jet flow behaviors and the interaction between jet and crossflow have been studied widely. Due to chaotic flow behavior, establishing of a mathematical model could not possible to accurately predict the flow field. Therefore, most of the study about JICF relied on computational fluid dynamic (CFD) and/or experimental methods.

There was plenty of the study results that proposed by the previous researcher. Some of research papers that used CFD method to simulate jet-crossflow interacting flow behavior are shown as followed. Yuan *et al.*, [1] proposed the study results of flow behavior of circular jet, varying the jet-crossflow velocity ratio, VR=2.0 and 3.3. The results showed that jet stream moving path coincided

---

* *Corresponding author.*
E-mail address: niohpuzu@gmail.com (Ni-oh Puzu)

with the power law fit, and the position, which the jet started bending to the crossflow direction, is located where the high inducing crossflow penetrated into the jet at the upstream region. Priere *et al.*, [2] studied the flow characteristic of two opposed rows of five in-line JICF at fixed VR=3.25 with installing baffle plates prior the jet exit. The results showed that the mixing process was improved by effecting of these plates to control the coming flow at the front of exit. Majander and Siikonen [3] used the Large Eddy Simulation technique to simulate JICF problem with maintaining VR=2.3. Their simulations showed well agreement with available experimental data. Behzad *et al.*, [4] reported the simulation results of liquid jet that was injected transversely into a high pressure gaseous crossflow with varying momentum flux ratio of 8, 10 and 15. The sheet-like structure was observed on the jet steam surface due to the effect of aerodynamic drag force of the crossflow. Esmaeili *et al.*, [5] improved the penetration, spread, inducement and mixing of the jet in crossflow properties by decreasing jet-crossflow temperature ratio under condition at VR=3.5. Zhang and Collins [6] presented the simulation results of vortex mechanism, which are addressed at VR=0.0-3.0, that was created from jet to affect the heat transfer surface at the downstream flow field. Ahn *et al.*, [7] numerically investigated the flow behaviors from two rows of film cooling holes with opposite orientation angles when the blowing ratio was varied of VR=0.5, 1.0 and 2.0. When the blowing ratio was 0.5, the results shown to achieve high film cooling effectiveness while increasing the injecting velocity tended to make vulnerable the effectiveness. Miao and Wu [8] also reported the simulation results about the effects of blowing ratios, varying from 0.3-1.5, and jet exit shape, which have influenced to film cooling effectiveness. The main results proposed that the thermal-flow field over the film-cooled plate dominated by strength of the Counter Rotating Vortex Pairs, CRVP, which was generated by the interaction of individual cooling jet and the crossflow.

In order to understand flow characteristics and validate simulation results, the experimental study is still indispensable. Huang and Jen Lan [9] captured the essential vortex types of JICF, due to shear flow between jet and mainstream, by projecting laser sheet through the vicinity area of the jet exit. The results explored that the 5 types of vortices can be seen in the range of VR=0.28-1.22. Moreover, the results were also proposed that the Strouhal number decayed exponentially with the increase of the VR. According to the results obtained from Kim *et al.*, [10], who also studied the flow adjacent the exit, which proposed the inducing effect mechanism from the jet stream by using the Particle Image Velocimetry (PIV) method. The experiments have been performed at VR=3.3 and two Reynolds numbers at 1,050 and 2,100, based on crossflow velocity and jet diameter. Compton and Johnston [11] presented experimental results of inclined jet to the mainstream, which studied in the range of VR=0.7-1.3. The results show that the produced vortices by the vortex generating jet were similar to vortices which was created by a solid vortex generator. Zhang [12] used rectangular jet exit to increase turbulence level of fluid inside the downstream boundary layer. The results showed that the rectangular jet was able to produce strong streamwise vortex same as a round jet. Lim *et al.*, [13] visualized the loop vortices and presented new understanding about the mechanism of forming vortices by setting flow condition at VR=4.6. The result showed that the vortex loops were not caused by the folding of the ring vortices. For the studies about the heat transfer applications [14-17], the configuration and condition of jet exits, e.g., VR, temperature, are also influence to heat transfer characteristics.

Although plenty of the study about JICF have been investigated, an experimentally study still limited to conduct the jet flow behavior at small velocity when compare to the mainstream flow. As a result, the jet flow attached on the surface which affect to heat transfer on the surface. So, the objective of the present study was focused to investigate flow behavior of JICF, especially effect of jet-to-mainstream velocity on flow behavior and CRVP to the jet structure.

2. Experimental Setup and Vital Details

For this study, the flow characteristics of jet in crossflow were investigated in water tunnel and wind tunnel. The details of the experimental setup and the measurement techniques including data processing were described in Section 2.1 and to 2.2. The experimenting results represented both qualitative and quantitative investigations of developing flow structure of the jet stream after interacting with the crossflow. The investigations of flow characteristics were conducted with different jet-crossflow momentum flux ratios, $J = \rho_j V_j^2 / \rho_m V_m^2$ having 5 values, 0.01, 0.06 0.25 1.0, 2.25, 4.0 and 12.25. While the crossflow velocity was kept the same. Here, ρ and V represented water density and fluid velocity, respectively. The subscript j and m indicated to jet and crossflow, respectively. For this experiment, ρ_j and ρ_m were considered the same density using same fluid.

2.1 Water Tunnel

Water tunnel has been designed and fabricated to study the jet structure development after interacting with the crossflow, focusing on CRVP structure in jet cross section. The schematic diagram of the experimental setup is shown in Figure 1. The water tunnel was made of clear glass plates and had a cross section area of 285x440 mm^2 and 3,700 mm in length. The water flow was circulated by 1.5 HP centrifugal water pump and the velocity of water flow in the tunnel was controlled by ball valve which located at the discharge side of the pump. In order to mitigate the turbulence flow in water tunnel, the pipe exit was covered by cotton bag before passing through the perforated plate and flow straightener, whereas suction side was a pipe to minimize pressure drop of the pump circuit. The uniform crossflow velocity in upstream region of test section was kept at 30 mm/s, Re=3,400, while the depth of water in channel was 350 mm. The jet flow rate was set to control jet-crossflow momentum flux ratios of J = 0.01, 0.06, 0.25, 1.0, 2.25, 4.0 and 12.25 before injecting downward from the exit. The flat plate in test section, which was made from acrylic flat plate, having 280 mm wide and 800 mm long and 10 mm thick, had a sharp leading (the angle of the lower edge was 15 degree) to keep an initial laminar flow near the leading edge. The plate was set horizontally in the central region of the channel as shown in Figure 1. The outlet of the jet pipe, with having a diameter D of 11 mm, was mounted at-grade to the surface in front of downstream surface. The jet exit was placed at 400 mm from the leading edge and distanced 150 mm from the bottom of the tunnel. For the present study, the origin of the Cartesian coordinate system was set at the downstream lip of the exit. To visualize jet stream structure after interacting with crossflow, water jet was mixed with fluorescence, Rhodamine B which was added in the jet fluid illuminating particle, before injecting into crossflow. Then the light sheet of argon-ion laser was projected perpendicular to the crossflow to visualize the jet stream structure.

Jet structure was captured by CCTV camera (Sony HP-9531PE) which was installed outside the tunnel with 45-degree respecting to the crossflow direction. For capturing on various plane with the same picture scale, CCTV camera and laser source were installed on the same movable XY table which was placed parallel to the tunnel.
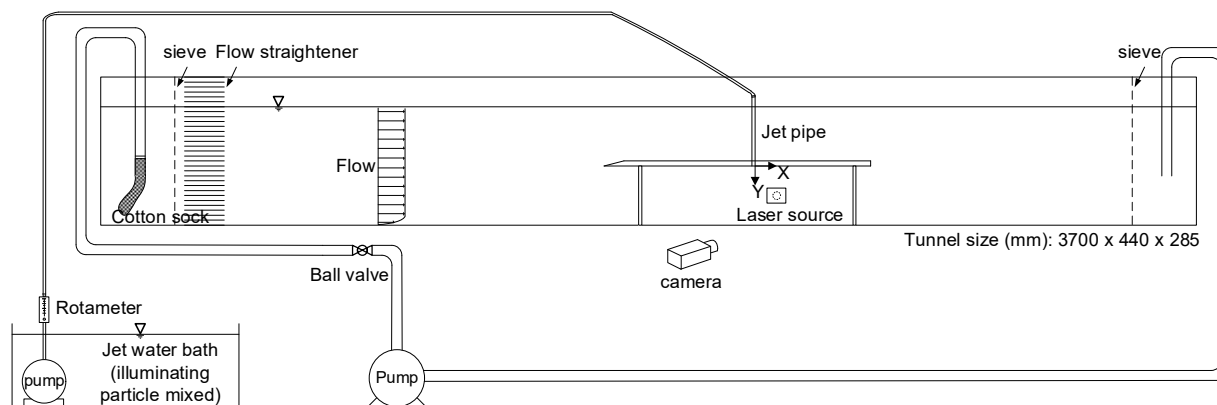
Fig. 1. Experimental setup of water tunnel

2.2 Wind Tunnel

The bell-shaped open flow wind tunnel, with a 400 mm x 400 mm square exit, was used to blow the crossflow over the flat plate with vortex generating jet nozzle. The details of the test section were shown in Figure 2(a). At the tunnel outlet, the uniform air velocity, V_m, was controlled at 10.0 m/s, which had 4.5% of turbulence intensity, and temperature was set at 26.0±0.2 °C for all experiments, while experiment room temperature was set at 24.0 °C.

The flat plate, which made of acrylic plate, 480 mm wide, 800 mm long and 20 mm thick, has a sharp leading (the angle of lower edge is 15 degree). The exit of the jet pipe with a diameter D of 14 mm was mounted to the surface of flat plate at a distance of 400 mm from the leading edge. A trip wire with 1.5 mm in diameter was attached at 14 mm from the leading edge to trig and accelerate turbulent boundary layer flow before location of jet nozzle [18]. The length of the aluminum jet pipe was 140 mm to achieve a fully developed flow at the jet exit. At the jet nozzle position, the boundary layer thickness was measured to be 14.14 mm. Based on the distance x from the leading edge of the test plate to the jet exit, the streamwise Reynolds number, $Re_x = V_m x/\upsilon$, was approximately 2.5 x 10^5. The kinematic viscosity, υ, was mostly constant for both streams.

For the jet trajectory investigation, the air jet was mixed with smoke generated by burning paraffin oil before injecting into the crossflow. Two CCD cameras were placed at the lateral side and the top of the flat plate to capture the jet path from the side and top view. In this experiment, the J values were also kept the same as water jet experiment of 0.01, 0.06, 0.25, 1.0, 2.25, 4.0 and 12.25, which corresponded jet Reynolds number, $Re_j = V_j D/\upsilon$ of 0.9 x 10^3, 2.2 x 10^3, 4.5 x 10^3, 9.0 x 10^3, 1.3 x 10^4, 1.8 x 10^4 and 3.1 x 10^4, respectively. When the crossflow air and the jet air were set the same temperature, the effect of density ρ of both streams was negligible.

For quantitative measurement of temperature distribution, jet stream was heated to 55.0 °C before injecting into the crossflow while the details of the flat plate and experimental condition were similar to the jet trajectory investigation. Temperature distributions on the jet cross section were measured at different downstream locations by using six of type-T thermocouples, as shown in Figure 2(b). The 40 AWG thermocouple wires (OMEGA®) were inserted into needles which had external diameter at 1.5 mm and placed at pitch distance of 5 mm. Row of the thermocouples was moved across the crossflow direction and parallel to the surface (measuring in the YZ plane). The holding rod of the sensors was fixed to the computer controlled XYZ table. The resolutions of temperature measurement on Y and Z direction were 2 mm and 1 mm, respectively. To evaluate reliable time-average temperature, the number of captured temperature data had to be sufficient to reduce the

effect of jet fluctuations. In this experiment, each position of temperature magnitudes was obtained from an average of 20 data recorded over 20 s. The results were then evaluated spreading and mixing characteristics of the jet stream after interacting with crossflow.

In order to investigate the jet spreading after interacting with the crossflow along downstream direction, dimensionless temperature, θ, was employed to consider jet cross section pattern, as defined in Eq. (1),

$$\theta = \frac{T - T_m}{T_j - T_m} \tag{1}$$

where T was an average temperature at the measured points, T_j and T_m were jet and crossflow temperatures at the exit, respectively.
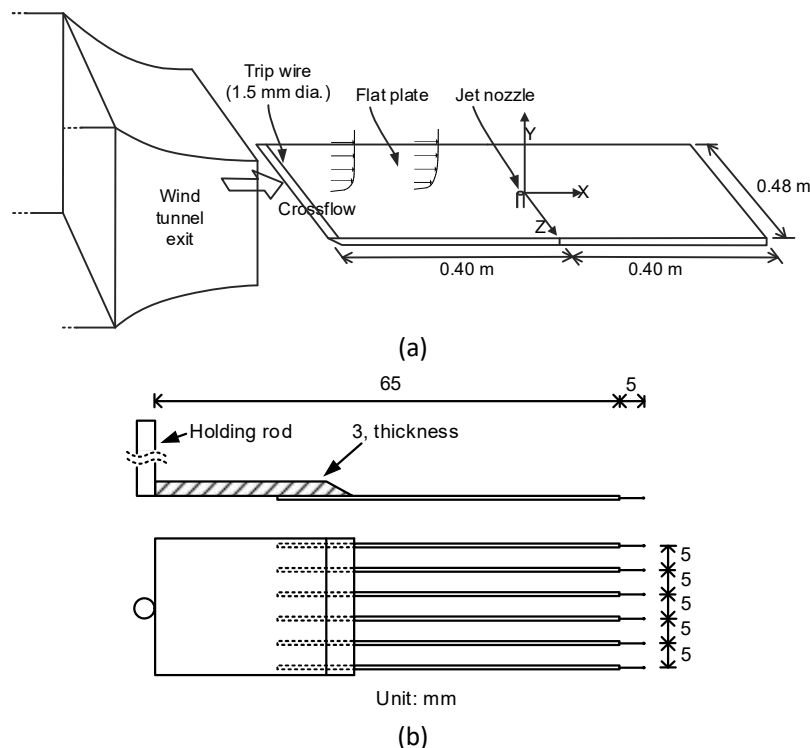

Fig. 2. Experimental setup of wind tunnel (a) Test section (b) temperature sensor configuration

3. Results and Discussion

3.1 Flow Structure in Jet Cross Section

Flow structure in cross section of the jet stream are changed as going downstream following to jet-crossflow momentum flux ratio, J as illustrated in Figure 3.

For $J = 0.01$, when the jet stream moves closely to the flat plate surface, jet structures display an opaque area as a dome-shape. As a result, it is shown that the unity flow of jet stream takes place, less inducing crossflow into the jet, which present at near field. When jet stream moves further, Counter Rotating Vortex Pairs, CRVP, gradually emerge inside the jet structure and represent the induced crossflow flowing into it. At the distances, $X/D \geq 5$, the non-uniform jet structure
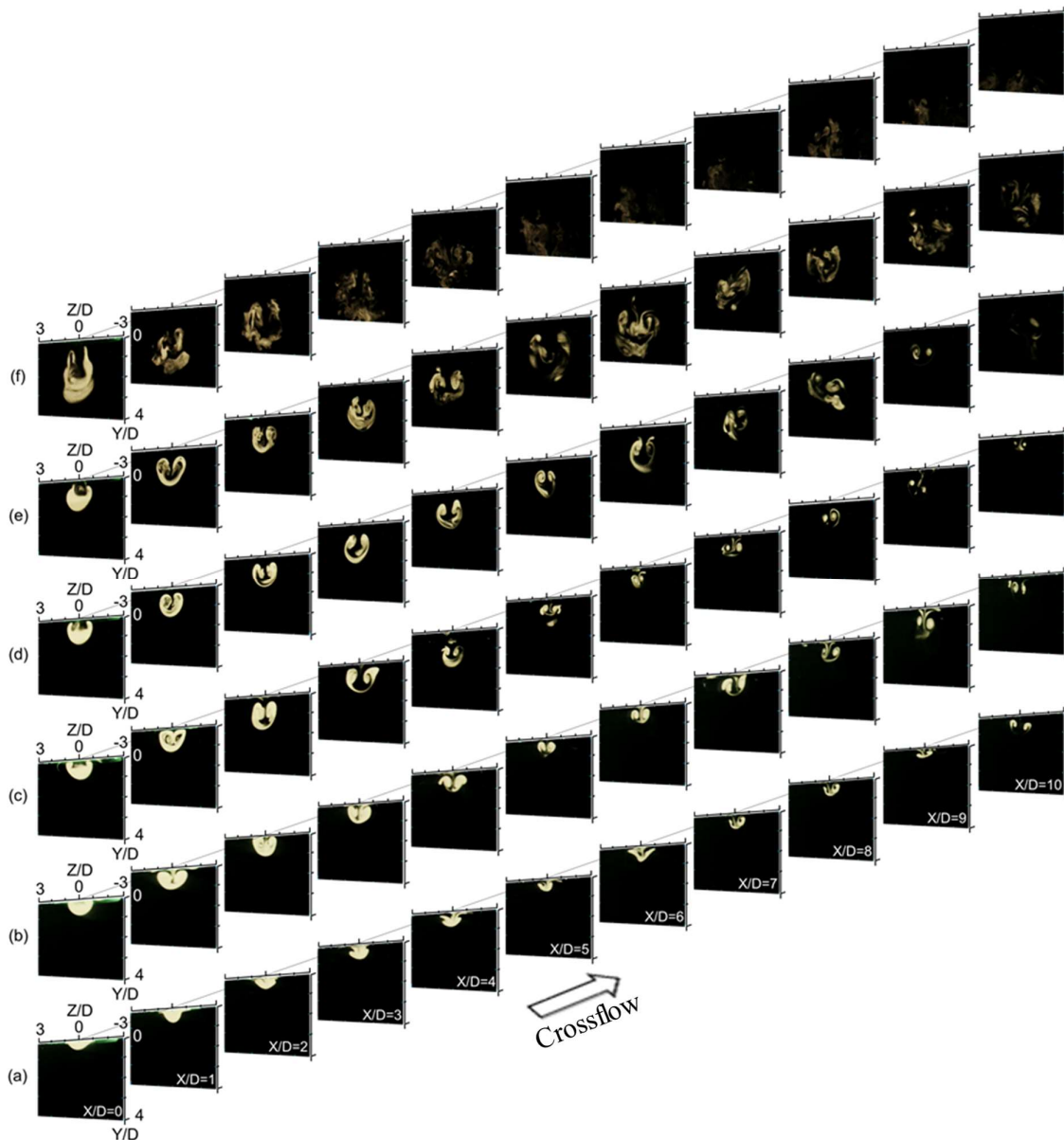
Fig. 3. Cross section of jet structure along downstream direction with various jet-crossflow momentum flux ratios, J: (a) 0.01, (b) 0.06, (c) 0.25, (d) 1.0, (e) 2.25, and (f) 4.0

distributions show the positions of CRVP rotating centers. At the distance from the jet exit, X/D=10, the jet structure can still be seen the near the plate which resists to mix with crossflow.

For J=0.25, jet stream can penetrate deeper to the crossflow and shows the higher turbulent motions inside the structure. The kidney-shape appears suddenly in the jet structure at X/D=1 because CRVP accelerates mixing process by entraining more neighboring fluid into the jet structure. From the observation of the flow field, the strength of CRVP increases according to the J values which more induce neighboring fluid upward between rotating centers, as show in Figure 3(b) at X/D=1. Although jet mass flow rate of J=0.5 is 2 times of J=0.25, the investigations of jet structure imply to show the similar size of jet structure. It can be concluded that the jet with higher J will be more spread and mix more strongly with ambient flow. From this behavior, the jet structure with higher J is expanded in any directions on investigation plane due to well spreading and mixing.

Nevertheless, the centers of rotating vortex still maintain the less mixing positions for each plane**.** At far position from the exit in the case of further increasing jet velocity, J=2.25, the jet structure, CRVP, cannot be captured due to high turbulence of interacting flow.

For further increasing J =4.0, while jet stream deeply penetrates and fast spread into the crossflow accompanying with highly turbulence interaction, the chaotic interaction flow is still captured as shown on plane at X/D=0-3. More severe interaction flow makes unable to identify the chaotic flow structures along downstream direction where the strong mixing process is taking place at the beginning.

3.2 Smoke Flow Visualizations

From the previous session, it is clearly shown that the J indicates substantial influence to the jet penetration ability, and this result continue affects to the jet trajectory as shown in Figure 4**.** The side views of flow are shown as the jet trajectory inside the crossflow with varying J of 0.01, 0.06, 0.25, 1.0, 2.25, 4.0 and 12.25. After the jet is injected from pipe exit, the jet stream is deflected by the crossflow to downstream direction, as in the case of a conventional transverse jet, showing the expanding of jet size and moving path.

For J=0.01, the moving jet attaches to the surface immediately after leaving from the jet exit because lower momentum of jet is dragged by crossflow which has higher momentum**.** When J is increased, it is observed that the jet trajectory still remains the same flow behavior and contacts to the surface except the distance of the jet stream from flat plate is higher due to the large spreading of jet flow. When jet velocity is increased corresponded to J=1.0, the jet flow departs from the plate
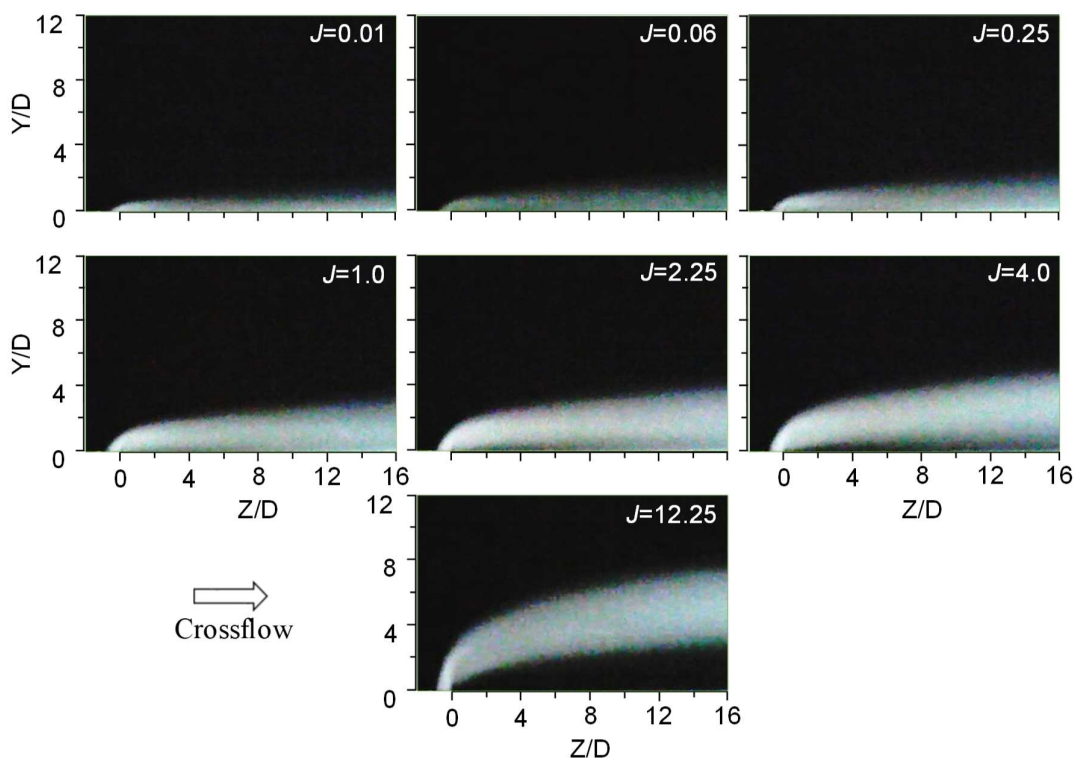

Fig. 4. Jet trajectory on the side view of flat plate

near the jet exit and show the reattachment flow behavior at X/D=10. This phenomenon has been clearly observed when the jet velocity increased corresponded to J=1.5.

For J=4.0, jet stream gradually lifts away from surface. It is reasonable to conclude that the jet stream has no direct influence to the adjacent surface fluid.

For J=12.25, jet stream lifts away from the surface, and dense jet fume was observed at the position that jet is being bent. The immediately changing of jet density was explained by Yuan and street [1] because entrainment effect on the windward region and effect of the loop vortex are enhanced by intruding deeply of crossflow into the jet.

For thoroughly understanding of jet trajectory characteristics, Figure 5 shows jet trajectory on the top view. For J=0.01, 0.06 and 0.25, jet stream flows parallel to the crossflow and have gradually expansion to compare with the exit diameter. In contrast for J=2.25, the stream suddenly expands to the lateral side after passing through exit and proposes the size further increasing along downstream, reaching about $4D$ width of jet band at X/D=16. Moreover, low-dense area adjacent to exit along downstream at jet centerline is observed and becomes more apparent after increasing the jet velocities, J=4.0 and 12.25. This behavior coincides with the position of upward flow in jet cross section, see in Figure 3, where neighboring fluid is entrained by the CRVP. The results of the jet trajectory from the top view show clearly that the smoke concentration inside the jet structure is non-uniform, especially when jet is presented at high J conditions. It should be noted here that the results of the jet trajectory as a single line from the previous studies [1,4,19–22] should be reminded that the highly dense jet area occurs on the lateral of jet centerline along downstream, so it seems only reasonable to use on the low jet velocity. The only single line trajectory from the side view might be misunderstanding the highest density lying down along center plane, Z/D=0.
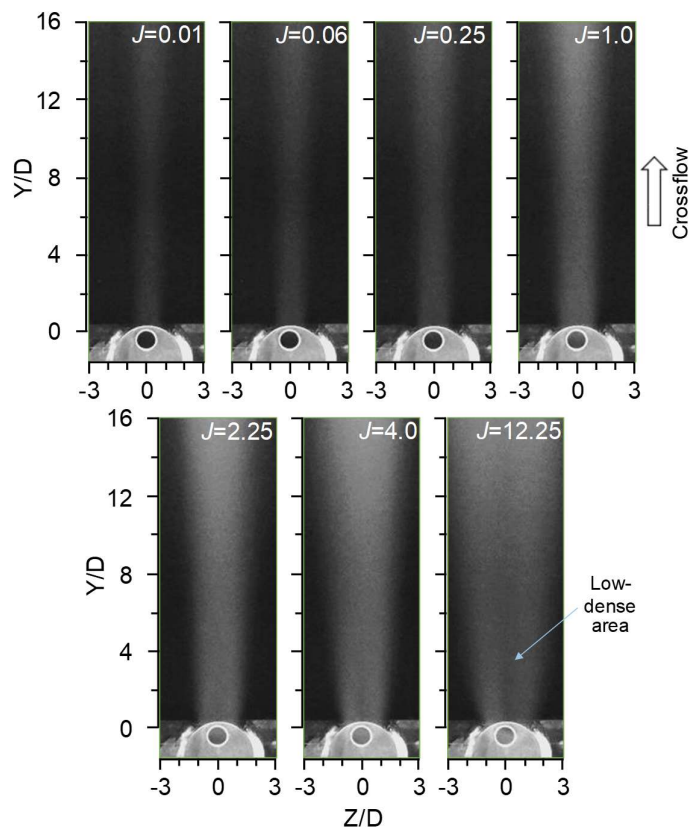

Fig. 5. Jet trajectory on the top view

3.3 Dimensionless Temperature Distributions

Figure 6 shows the dimensionless temperature distribution, θ, inside jet structure on the perpendicular plain to the crossflow. The distribution patterns of J=0.06 looks like dome-shape, which have the highest value, θ=0.26, at the innermost region closing to the surface while temperature continuously decrease to the outside. At X/D=6, the base of jet structure covers $4D$ width with $1.8D$ tall which considered at contour boundary of θ=0.02. To consider the farther distances, the jet distribution still maintains dome-shape pattern. While cross section area is being increased due to mixing process occurring along jet path, the highest value continues to decline. From the previous experimental results is being remembered that the CRVP also takes place for jet moving close to the surface (see Figure 3). the θ values distributions show layer by layer of interior structure without kidney-shape pattern. It can be concluded that the entrainment fluid from the bottom is being blocked. This phenomenon leads to be invisible the kidney-shape pattern inside the structure.

For the case of jet lifts away from the surface, J=12.25, the boundary of the jet structure has about circular shape, but the distribution inside the structure gradually changes and becomes to the kidney-shape that representation the entrainment fluid is influenced to shape pattern and also indicate that the innermost layer still maintains the less mixing region. At the innermost layer at X/D=2, the θ is approximate 0.30. Note that the bottom curve of the kidney-shape coincides with the upward flow fluid in which CRVP entrains the neighboring fluid into the jet stream. It is concluded that the entrainment fluid plays important role in the kidney-shape appearance, especially for the jet penetrating deeply into the crossflow. As the conventional behavior of jet dilution tends to decrease along the downstream, jet area spread widely to the lateral side due to much higher of jet flow rate.

The influence of the J with according to the distance from the exit to decaying of dimensionless temperature is shown in the Figure 7. As the results have been described, the injection velocity is increased, namely J. The rotating speed of CRVP will also enhance due to high energetic jet stream. For J=0.06 at X/D=2, low velocity jet is pressed by the coming crossflow to form the difference contour shapes that representation of decaying process is taking place while jet moves along downstream. For the results of J=2.25 and 12.25, decaying pattern differ from the lower one, but kidney-shape regions still indicate the place where jet fluid well resists to mix with neighboring fluid. In order to compare the rate of decay, higher J shows that the jet stream needs to take longer distance to engulf by crossflow.

Figure 8 shows the decreasing values of θ_{max}, which is represented to decaying rate relating to the traveling distance. As expecting results, θ_{max} at the exit is unity. It is observed that the higher decline rate of θ_{max} occurs at the near field where the interval of jet is bending. While J=0.06 shows the highest incline rate at the beginning of the interaction of fluids, the differences of decay rates have little value for the cases J=2.25 and 12.25. At X/D=16, the θ_{max} for J=12.25 maintained the highest value. It indicates that the higher injecting velocity jet confirms to need the longer travelling distance to merge into the crossflow.
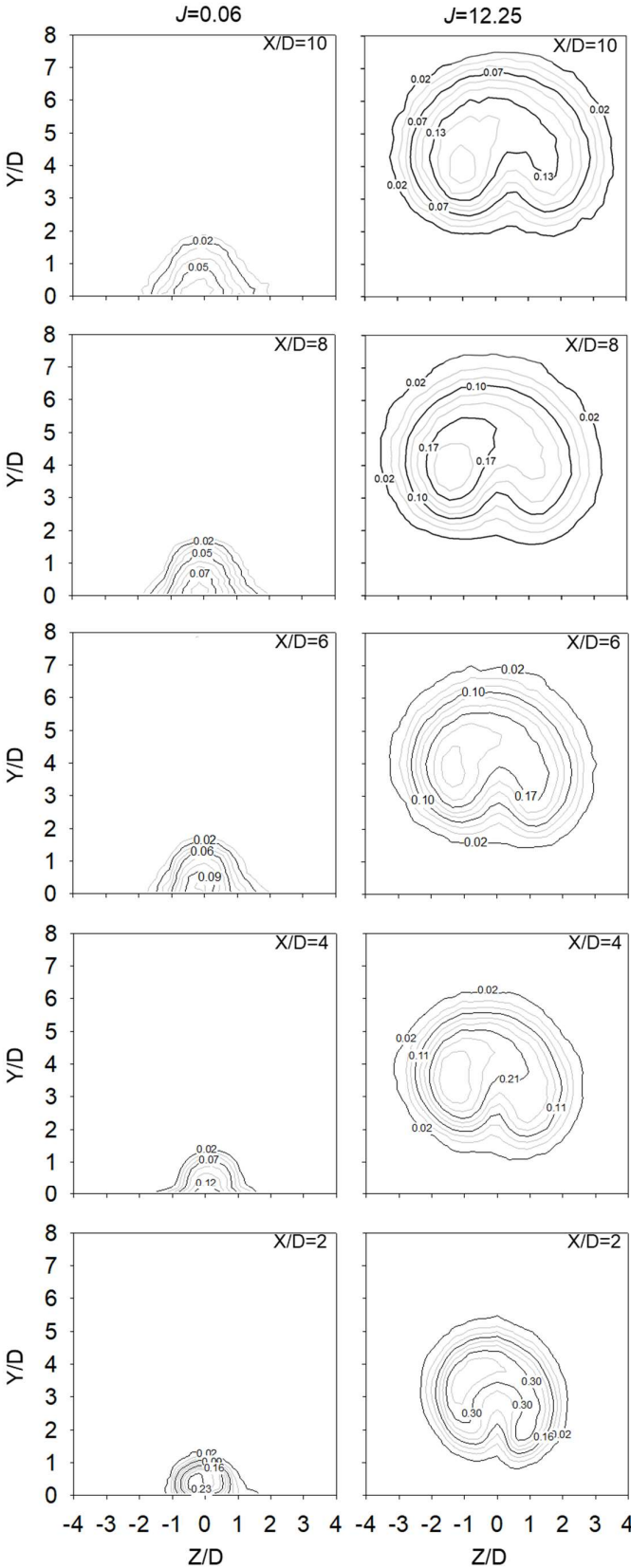
Fig. 6. Dimensionless temperature distribution at different downstream planes for J=0.06 and 12.25
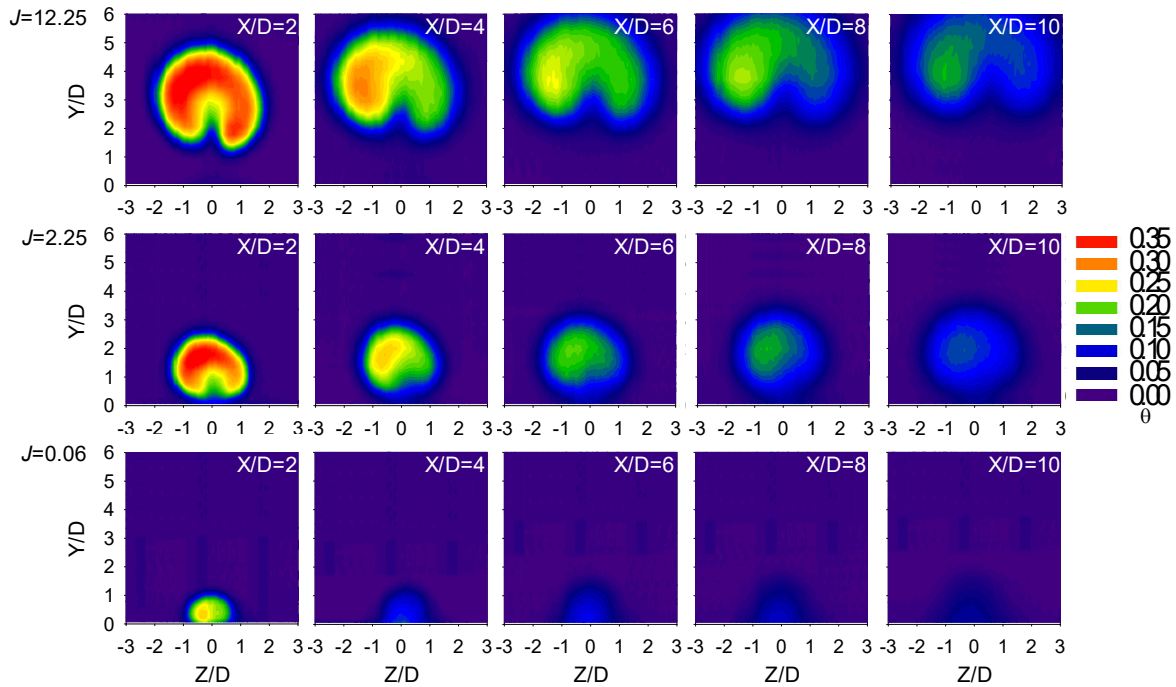
Fig. 7. Decaying of dimensionless temperature at different downstream planes for J=0.06, 2.25, and 12.25
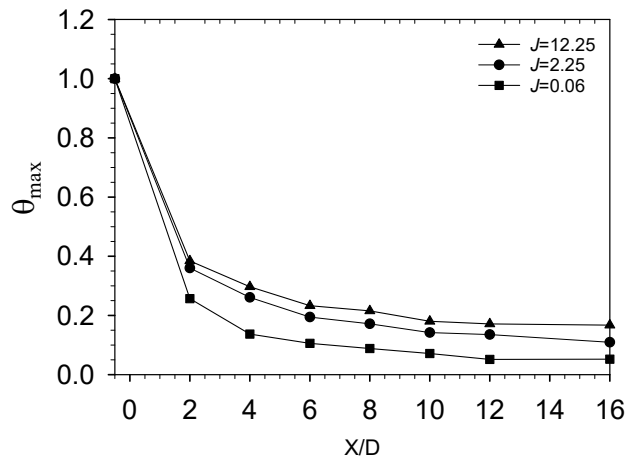

Fig. 8. Jet decaying along downstream

Figure 9 represents the dimensionless of the expansion jet cross section area that is calculated from θ value, as defined in Eq. (2)

$$A^{'} = A_m/A_j \tag{2}$$

where A_m represents the cross-section area that is measured from the temperature distribution, taking θ≥0.02 to calculate the area, and A_j is the area of the jet exit. For J=0.06, jet cross section area is just little bigger than the exit, which the size keeps almost constant along downstream direction. After X/D=16, the jet size becomes smaller. For J=2.25 at after X/D=2, jet cross section area rapidly increases about 5 times of jet exit area, which shows that the beginning of the interaction accelerates

171

the spreading phenomenon. And at X/D=16, the jet area is increased approximately to 10 times of the jet exit. For the highest jet velocity J=12.25, jet area is more expanded due to high jet stream flowrate, and high turbulence is achieved at the beginning of the interaction. This effect leads the X/D=2 position to increase the area about 10 times of the jet exit, and at X/D=16 reaches to 33 times.
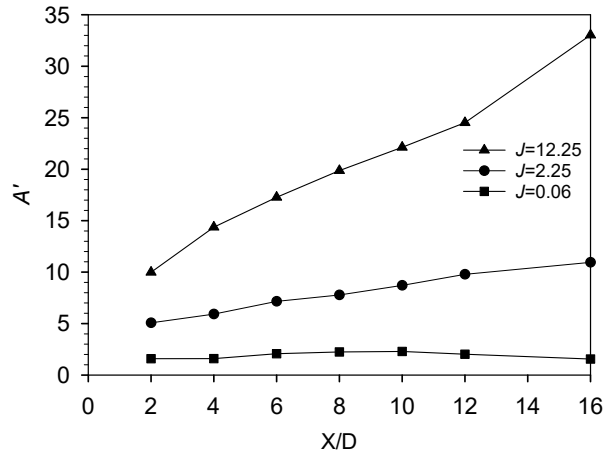

Fig. 9. The expansion of dimensionless jet cross section area

Finally, the correlation has been developed to predict the values of dimensionless jet cross section area in the following,

$$A'_{pre} = J^2(-0.0069 - 0.007X) + J(1.306 - 0.208X) - 0.003X + 1.761 \qquad (3)$$

where X refers to the X/D distances. The prediction values of Eq. (3) lie with in ±15% of the experimentally observed data values. Therefore, the correlation developed can predict the values of dimensionless jet cross section area with reasonable accuracy in the range of acceptable.

4. Conclusions

The jet structures after interacting with the crossflow have been investigated experimentally by conducting the water tunnel to visualize water jet at low Reynold number flow and wind tunnel to visualize the spreading temperature on the downstream normal plane and capture the jet trajectory. The effect of CRVP and jet-crossflow momentum flux ratio, J, to jet structure pattern were explored. The main conclusions of experimental results are as below.

i.   Dome-shape structure of the jet stream occurs at the case of jet moving contact to the surface. When the injecting velocity, or J, is increased, the CRVP will clearly show and imposes the faster of rotating speed.

ii. In the case of flow attaching with the surface, J=0.01, 0.06, and 0.25, the innermost region inside jet structure maintains the highest temperature, and kidney-shape is invisible because the entrainment fluid from the CRVP at the underneath is being blocked. For jet lifting flow, J=1.0, 2.25, 4.0 and 12.25, the kidney-shape is formed by the CRVP to entrain the neighboring fluid flowing upward at the center plane while the innermost regions of kidney-shape still have the highest temperature region, less mixing area.

iii. The mixing process is taking place along the jet path, so the jet temperature will be decreased until it is engulfed by the crossflow. Although the higher jet velocity, J, mixing performed well due to jet rapidly spread to the lateral after chaotic interacting, the process still needs the longer moving distance to dilute the high mass flow rate jet.

Acknowledgements

References

[1]   Yuan, Lester L., and Robert L. Street. "Trajectory and entrainment of a round jet in crossflow." *Physics of fluids* 10, no. 9 (1998): 2323-2335.
[2]   Priere, C., L. Y. M. Gicquel, P. Kaufmann, W. Krebs, and T. Poinsot. "Large eddy simulation predictions of mixing enhancement for jets in cross-flows." *Journal of Turbulence* 5, no. 005 (2004): 1-24.
[3]   Majander, Petri, and Timo Siikonen. "Large-eddy simulation of a round jet in a cross-flow." *International Journal of Heat and Fluid Flow* 27, no. 3 (2006): 402-415.
[4]   Behzad, M., N. Ashgriz, and B. W. Karney. "Surface breakup of a non-turbulent liquid jet injected into a high pressure gaseous crossflow." *International Journal of Multiphase Flow* 80 (2016): 100-117.
[5]   Esmaeili, Mostafa, Asghar Afshari, and Farhad A. Jaberi. "Turbulent mixing in non-isothermal jet in crossflow." *International Journal of Heat and Mass Transfer* 89 (2015): 1239-1257.
[6]   Zhang, Xin, and Michael W. Collins. "Flow and heat transfer in a turbulent boundary layer through skewed and pitched jets." *AIAA journal* 31, no. 9 (1993): 1590-1599.
[7]   Ahn, Joon, In Sung Jung, and Joon Sik Lee. "Film cooling from two rows of holes with opposite orientation angles: injectant behavior and adiabatic film cooling effectiveness." *International Journal of Heat and Fluid Flow* 24, no. 1 (2003): 91-99.
[8]   Miao, Jr-Ming, and Chen-Yuan Wu. "Numerical approach to hole shape effect on film cooling effectiveness over flat plate including internal impingement cooling chamber." *International Journal of Heat and Mass Transfer* 49, no. 5-6 (2006): 919-938.
[9]   Huang, Rong F., and Jen Lan. "Characteristic modes and evolution processes of shear-layer vortices in an elevated transverse jet." *Physics of Fluids* 17, no. 3 (2005): 034103.
[10] Kim, K. C., S. K. Kim, and S. Y. Yoon. "PIV measurements of the flow and turbulent characteristics of a round jet in crossflow." *Journal of visualization* 3, no. 2 (2000): 157-164.
[11] Compton, Debora A., and James P. Johnston. "Streamwise vortex production by pitched and skewed jets in a turbulent boundary layer." *AIAA journal* 30, no. 3 (1992): 640-647.
[12] Zhang, X. "An inclined rectangular jet in a turbulent boundary layer-vortex flow." *Experiments in Fluids* 28, no. 4 (2000): 344-354.
[13] Lim, T. T., T. H. New, and S. C. Luo. "On the development of large-scale structures of a jet normal to a cross flow." *Physics of fluids* 13, no. 3 (2001): 770-775.
[14] Beniaiche, Ahmed, Adel Ghenaiet, and Bruno Facchini. "Experimental and numerical investigations of internal heat transfer in an innovative trailing edge blade cooling system: stationary and rotation effects, part 1—experimental results." *Heat and Mass Transfer* 53, no. 2 (2017): 475-490.
[15] Fénot, M., E. Dorignac, and G. Lalizel. "Heat transfer and flow structure of a multichannel impinging jet." *International Journal of Thermal Sciences* 90 (2015): 323-338.
[16] Johnson, Blake, Wei Tian, Kai Zhang, and Hui Hu. "An experimental study of density ratio effects on the film cooling injection from discrete holes by using PIV and PSP techniques." *International Journal of Heat and Mass Transfer* 76 (2014): 337-349.
[17] Liu, Cun-liang, Hui-ren Zhu, Jiang-tao Bai, and Du-chun Xu. "Film cooling performance of converging slot-hole rows on a gas turbine blade." *International Journal of Heat and Mass Transfer* 53, no. 23-24 (2010): 5232-5241.
[18] Abu-Mulaweh, H. I. "Experimental investigation of the influence of buoyancy on turbulent flow adjacent to a horizontal plate induced by a trip wire." *International journal of thermal sciences* 42, no. 11 (2003): 1013-1020.
[19] Karagozian, Ann R. "The jet in crossflow." *Physics of Fluids* 26, no. 10 (2014): 1-47.
[20] Eroglu, Adnan, and Robert E. Breidenthal. "Exponentially accelerating jet in crossflow." *AIAA journal* 36, no. 6 (1998): 1002-1009.

[21]   Sakai, E., T. Takahashi, and H. Watanabe. "Large-eddy simulation of an inclined round jet issuing into a crossflow." *International Journal of Heat and Mass Transfer* 69 (2014): 300-311.
[22]   Wegner, B., Y. Huai, and A. Sadiki. "Comparative study of turbulent mixing in jet in cross-flow configurations using LES." *International Journal of Heat and Fluid Flow* 25, no. 5 (2004): 767-775.